9-15-2004

Optical properties of SiO$_X$ nanostructured films by pulsed-laser deposition at different substrate temperatures

X. Y. Chen
National University of Singapore

Yongfeng Lu
University of Nebraska-Lincoln, ylu2@unl.edu

Y. H. Wu
National University of Singapore

B. J. Cho
National University of Singapore

W. D. Song
Data Storage Institute, 5 Engineering Drive 1, Singapore 117608, Singapore

See next page for additional authors

Authors

X. Y. Chen, Yongfeng Lu, Y. H. Wu, B. J. Cho, W. D. Song, and D. Y. Dai

Optical properties of SiO$_x$ nanostructured films by pulsed-laser deposition at different substrate temperatures

X. Y. Chen
Department of Electrical and Computer Engineering, National University of Singapore, 10 Kent Ridge Crescent, Singapore 119260, Singapore

Y. F. Lu[a)]
Department of Electrical Engineering, University of Nebraska, Lincoln, Nebraska 68588-0511

Y. H. Wu and B. J. Cho
Department of Electrical and Computer Engineering, National University of Singapore, 10 Kent Ridge Crescent, Singapore 119260, Singapore

W. D. Song and D. Y. Dai
Data Storage Institute, 5 Engineering Drive 1, Singapore 117608, Singapore

Silicon oxide (SiO$_x$) nanostructured films have been formed by pulsed-laser deposition of Si in oxygen at different substrate temperatures, in order to study the structures and optical properties related to quantum confinement effects. After laser ablation, the single-crystal Si(100) target is converted to a polycrystal structure and shows weak photoluminescence (PL). The as-deposited SiO$_x$ nanostructured films show large particles (i.e., droplets) on a uniform background film. The droplets with weak PL emission have the same high crystallinity as the Si(100) target. Strong PL is observed from the amorphouslike background films rather than from the crystalline droplets. As substrate temperatures increase from room temperature (23 °C) to 800 °C, the PL band continually redshifts from 1.9 to 1.6 eV and the optical band gap decreases from 2.9 to 2.1 eV due to the increased Si concentration in the films. After high-vacuum annealing at 800 °C, both the PL and optical absorption are enhanced. The optical band gap also decreases after annealing. Combined with the progressive PL redshifts of the SiO$_x$ films with increasing Si concentration by plasma-enhanced chemical vapor deposition, the results support the quantum confinement theory. © *2004 American Institute of Physics.* [DOI: 10.1063/1.1782274]

I. INTRODUCTION

Bulk silicon (Si) has an indirect band gap and is inefficient as a light source for optoelectronic applications. Ever since visible photoluminescence (PL) was observed in Si nanostructures,[1–3] Si nanocrystals (NCs) have generated much interest in microelectronics and optoelectronics. They have opened up opportunities for developing Si-based light emitting devices which are compatible with current electronic ultralarge-scale-integration technologies.

Si NCs have been synthesized by several techniques such as microwave-induced or laser-induced decomposition of silane (SiH$_4$)-like precursors,[2,4] ion implantation of Si$^+$,[5] electrochemical etching of Si wafers,[6] low pressure chemical vapor deposition,[7] plasma-enhanced chemical vapor deposition[8] (PECVD), and pulsed-laser deposition (PLD) of Si.[9] Si NCs ranging from 2 nm to tens of nanometers in size have been obtained successfully. The ability to control the size, surface condition, and doping of Si NCs with reproducibility is critical due to the sensitive light emitting properties of Si NCs.

Among the fabrication methods, PLD is a promising technique due to its ability to control size distribution and maintain crystal purity in a cold-wall ambient.[10] With this method, the size distribution of Si NCs can be flexibly controlled by varying background gas species and pressure,[11] laser fluence,[12] target-to-substrate distance,[13] and post annealing or oxidation.[14] The as-deposited Si NCs often show stoichiometries of Si oxide (SiO$_x$, $0 < x < 2$) due to the strong reaction of Si with residual oxygen in the chamber during the expansion of the Si plasma plume.[15] In this study, we examined the influence of substrate temperatures on the structures and properties of SiO$_x$ nanostructured films formed by PLD, as substrate temperature is a key parameter in determining film-substrate interaction and controlling film-cluster growth.

II. EXPERIMENTAL SETUP

SiO$_x$ nanostructured films were deposited in a Neocera PLD system. After laser ablation of the rotating Si(100) target at an incident angle of 45°, a luminescent Si plasma plume perpendicular to the target surface was generated and extended toward the substrates that were identical to the target. The hot ejected species (atoms, ions, cluster with a few atoms) with high kinetic energies in the plume were cooled down in ambient oxygen (O$_2$) gas and deposited on Si(100) or fused quartz (SiO$_2$) substrates. A pulsed KrF excimer laser (Lambda Physik 100, $\lambda = 248$ nm, $\tau = 30$ ns) was used as light source at a repetition rate of 10 Hz and a laser fluence of

a)Author to whom correspondence should be addressed; FAX: 402-472-4732; electronic mail: yflu@engr.unl.edu

3.0 J/cm^2. The target-to-substrate distance was ≈ 6 cm. The Si target was rotated constantly by an external motor to provide each pulse a fresh surface. The substrates were cleaned with acetone and ethanol ultrasonic baths before deposition. After the base vacuum was pumped down to 1.0 $\times 10^{-5}$ Torr, the substrates were resistively heated to fixed temperature. Then O$_2$ gas with 99.7% purity was introduced into the vacuum chamber and maintained at a constant pressure of 1 mTorr. With 30 min PLD, the thickness of the films was around 100 nm as measured by surface profiling. In this study, the substrate temperature varied from room temperature (23 °C) to 800 °C.

In luminescent Si plasma plume, large clusters will flight at a smaller angle from the target to substrate compared with small clusters, due to scattering by the ambient gas. Roughly speaking, large NCs are formed at the center of the plume, while the smaller ones are formed near the plume edge. Thus, larger NCs are deposited on the substrates which are near the plume center. In this work, all the samples were obtained at the plume center axis for consistency.

For comparison, PECVD SiO$_x$ films with a thickness of ~ 400 nm were deposited on Si(100) or fused quartz substrates in an Oxford PECVD system using rf (13.56 MHz) glow-discharge decomposition of very large-scale-integration (VLSI) grade 5% SiH$_4$ in nitrogen (N$_2$) carrier gas and VLSI grade 100% nitrous oxide (N$_2$O). Chamber pressure, rf power, total flow rate, substrate temperature, and deposition time were kept at 1 Torr, 20 W, 880 sccm, 300 °C, and 5 min, respectively. The flow ratio ($R = [N_2O]/[SiH_4]$) was varied between 20 and 1.

After deposition, the films were annealed *ex situ* in 10^{-8} Torr high vacuum for 60 min at a temperature of 800 °C.

The film structures were investigated by a Cu $K\alpha$ radiation ($\lambda = 0.154\,18$ nm) x-ray diffraction at room temperature. The PL and Raman spectra were recorded by a Renishaw micro-Raman and PL 2000 microscope (spatial resolution: ~ 1 μm) with an electrically cooled charge-coupled device detector at room temperature, using 514.5 nm Ar ion laser line as an excitation source. The surface morphology was observed using a Hitachi S-4100 field-emission scanning electron microscope. The nanostructural features were observed by plan-view high-resolution transmission electron microscopy (HRTEM) using a JEOL JEM-2010F field-emission electron microscope operated at 200 kV.

The surface composition was determined by x-ray photoelectron spectroscopy (XPS) with a Physical Electronics Quantum 2000 Scanning ESCA microprobe using a monochromatic Al $K\alpha$ (energy 1486.6 eV) radiation. Spectra were taken after 2 min sputter etching to remove surface contamination. The energies of XPS spectra were calibrated using the C 1s at a binding energy of 284.5 eV. Integrated peak area intensities under O 1s, Si 2p, and N 1s peaks were used for estimating the relative elemental composition of the films after correction of core-level atomic sensitivity factors.

The optical transmittance and reflectance were measured by a Shimadzu UV-3101PC spectrophotometer.
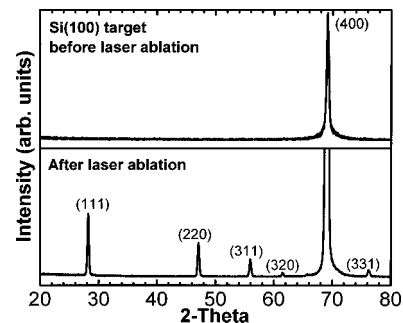

FIG. 1. XRD spectra of the Si(100) target before and after laser ablation in PLD.

III. RESULTS AND DISCUSSION

A. Target properties

The properties of the Si(100) target before and after laser ablation in PLD were examined. Figure 1 shows the XRD spectra of the target. Before laser ablation, the target shows a single-crystal structure with (100) orientation. After laser ablation, the multiple diffraction peaks indicate that the target surface was converted to poly-Si. The enhanced (400) diffraction peak also confirmed the better crystallinity. During laser ablation, the high laser fluence caused the inhomogeneous melting and ablation on the target surface. Local variations of the melting and crystallization rates resulted in rippling and roughing of the liquid-solid phase, especially at the phase boundary. Microstructures were formed, oxidized, and etched on the target surface by continuous laser pulses. The better crystalline poly-Si structure was due to the high temperature melting of the target surface during laser ablation.

Figure 2 shows the PL spectra of the target. Before laser ablation, there was no PL from the target, which is the expected result for the bulk crystalline Si (c-Si). After laser ablation, the target showed weak PL. However, the PL was not repeatable over the ablated area. The PL peak position and intensity varied greatly from region to region. During PLD, the collisions between the ejected species and the ambient gas determined the gas dynamics of the plume, inducing a backward flux of clusters that also deposited on the target surface. The enhanced PL may be from the deposited clusters. In addition, the oxidized microstructures formed on the target surface can give rise to PL. The microstructures were also ablated by the subsequent laser pulse to form
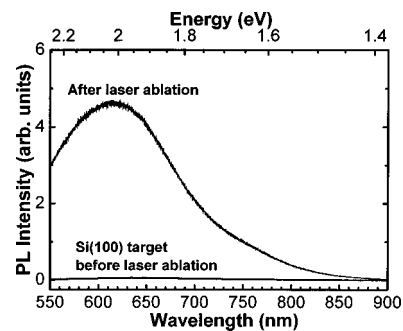

FIG. 2. PL spectra of the Si(100) target before and after laser ablation in PLD.
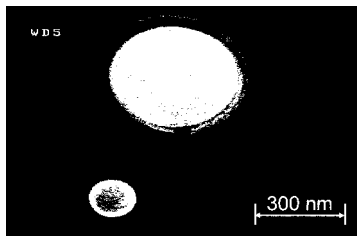
FIG. 3. SEM image of the SiO_x nanostructured film deposited by PLD at room temperature (23 °C).

ejected species. There is some correlation between the PL from the target and the deposited films.

B. Structure and composition of the deposited thin films

The surface morphology of the as-deposited SiO_x nanostructured films formed by PLD was observed by scanning electron microscopy (SEM). Figure 3 presents the image of the film deposited at 23 °C. The as-deposited film shows a large number of particles on a uniform background film. The particles with sizes from ~100 nm to several micrometers were droplets of target material deposited along with the film, which is an inherent drawback of PLD. It was also found that the films deposited at other elevated substrate temperatures showed a similar structure with droplets on a background film. In this paper, the background film is referred to as the droplet-free film region. As is well known, plume dynamics are greatly determined by gas pressure. At a gas pressure of 1 mTorr, there are few collisions between the ejected species before they reach the substrate, as the mean free path of the ejected species is ≈5 cm.[16] Therefore, solidified liquid droplets expelled from the target are predominant, while vapor species are deposited as a background film. The surface morphology does not change much at various substrate temperatures. On the contrary, the increase of gas pressure results in increased collisions between the ejected species and the ambient gas and causes a transition from a film structure to a porous cauliflowerlike structure, as the ambient gas pressure increases from 1 mTorr to 1 Torr.[17]

The nanostructural features of the as-deposited SiO_x nanostructured films formed by PLD were observed by HRTEM. Figure 4 shows the plan-view HRTEM image of the background film deposited at 23 °C. The absence of Si lattice planes indicates the amorphous state of the film. As
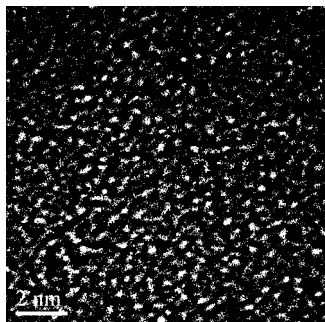

FIG. 4. Plan-view HRTEM image of the SiO_x nanostructured film deposited by PLD at room temperature (23 °C).
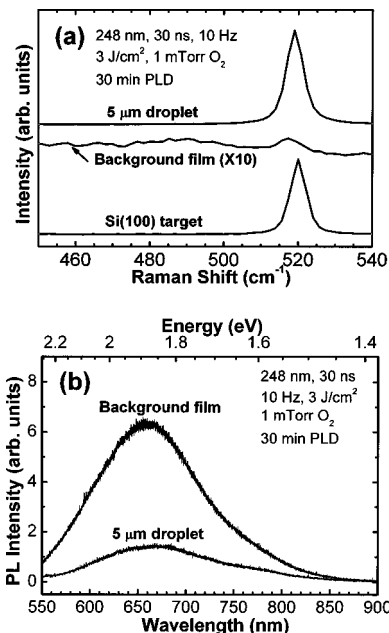

FIG. 5. The comparison of (a) Raman and (b) PL spectra of a 5 μm droplet and the background film deposited by PLD at room temperature (23 °C). The Raman spectrum of the Si(100) target is also shown for reference.

HRTEM is only sensitive to the presence of Si lattice planes, the presence of noncrystalline Si NCs cannot be confirmed by TEM measurements. At other elevated substrate temperatures up to 800 °C, all the deposited background films had a similar amorphouslike structure. In the PLD process, condensation of vapor during the fast expansion of Si plasma plume by laser ablation occurs under strong nonequilibrium conditions. A typical cooling rate for the plume expanding into vacuum reaches 10^{10}–10^{11} K/s.[18] Due to the lack of kinetic energy, all the impinged species essentially stick to the substrates. Le *et al.*[19] reported that in a 5–100 μs delay after ablation pulse, the SiO temperature decreases from around 2300 to 500 K in 100 mTorr Ar. As a consequence of rapid cooling, a metastable structure or amorphouslike structure is formed. Thus, subsequent annealing is necessary for a more stable structure and better crystallinity. It should be pointed out that the SiO_x films deposited by PECVD are also amorphous due to the low substrate temperatures (<500 °C).

The SiO_x nanostructured films formed by PLD were further characterized by micro-Raman and PL spectroscopy. Figure 5(a) shows the Raman spectra of a 5 μm droplet and the background film deposited at 23 °C. The Raman spectrum of the virgin Si(100) target is also shown for reference. The Raman peak of the target at 520 cm^{-1} corresponds to the TO phonon mode of the *c*-Si. The strong peak at 519 cm^{-1} in the Raman spectrum of the droplet indicates that the droplet has the same high crystallinity as the target. On the contrary, the Raman spectrum of the background film shows a weak crystalline peak at 517 cm^{-1} and a broadband at ≈480–500 cm^{-1} corresponding to the amorphous Si (*a*-Si). At other elevated substrate temperatures up to 800 °C, all the deposited background films were found to have the similar Raman spectra, which confirms the amorphous state of the films.
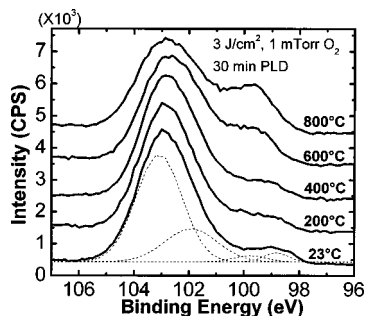
FIG. 6. Si $2p$ spectra of the SiO$_x$ nanostructured films deposited by PLD at different substrate temperatures.

FIG. 7. Si $2p$ spectra of the SiO$_x$ films deposited by PECVD at different values of flow ratio $R = [N_2O]/[SiH_4]$.

It is noticed that the Raman peak position is redshifted for some droplets but identical with that of the target for other droplets. The crystalline peak at 517 cm^{-1} of the background film is also redshifted and broadens compared to that of the target. According to the phonon confinement model given by Campbell and Fauchet,[20] the phonon confinement effects cause a redshift of Raman spectrum due to the size reduction of NCs, while the width of Raman spectrum is related to the size distribution of NCs. However, a quantitative analysis is difficult since the influence of the amorphous phase and the stresses in the film also need to be taken into account. The Raman peak will be redshifted and blueshifted by the tensile and compressive stresses, respectively.

Figure 5(b) shows the PL spectra of the droplet and the background film deposited at 23 °C. It was found that the droplets, as big particles, exhibited weak or no PL. The size of the droplets is too big to show the quantum confinement effect (QCE), although some of the droplets were formed by the coalescence of smaller droplets. On the contrary, a broad PL band at $\sim$1.9 eV was observed from the background film. The PL is therefore from the background film rather than from the droplets.

The composition of the SiO$_x$ films was characterized by XPS. It is now widely accepted that the Si $2p$ spectra can be interpreted in terms of five oxidation states: Si^0, Si^{1+}, Si^{2+}, Si^{3+}, and Si^{4+}. The network of SiO$_x$ is formed by Si-(Si$_{4-n}$-O$_n$) tetrahedra with $n=0-4$. From pure a-Si ($n=0$) for Si atom bonded to four nearest-neighbor Si atoms to a-SiO$_2$ ($n=4$) for Si atom bonded to four nearest-neighbor oxygen atoms, Si atoms are stepwise replaced by oxygen atoms with increasing oxidation states. The increasing electronegativity of the Si-O bond relative to the Si-Si bond results in a shift to higher binding energy of the core-level electrons in the Si. The binding energies for the progression of Si^0 to Si^{4+} range from $\approx$99.0 to 103.3 eV with a shift of $\sim$1 eV per Si-O bond.[21–23]

Figure 6 shows the Si $2p$ spectra of the SiO$_x$ nanostructured films deposited by PLD at different substrate temperatures. From the Si $2p$ spectrum of the SiO$_x$ film deposited at 23 °C, a broad curve with two peaks at $\sim$103.0 and 99.0 eV can be observed. Gaussian fitting reveals that the two peaks are composed of a superposition of different oxidation-state peaks. With increasing substrate temperatures, the higher energy peak (higher oxidation state) became weaker. The lower energy peak (lower oxidation state) became stronger with
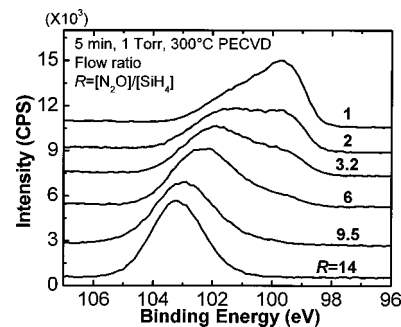
shifts to higher binding energy. The increase of the peak ratio of the lower energy peak over the higher energy peak reveals that the Si is less oxidized, or more oxygen is depleted, with increasing substrate temperatures. The composition changes are attributed to the absorption, diffusion, and desorption processes at the film/substrate interface. The substrate temperature is a key parameter in determining the free energy of film-atom clusters and thus the balance between the absorption, diffusion, and desorption processes. The surface mobility is higher at higher temperatures. On the other hand, material desorption becomes easier at higher temperatures. As a result, the deposited film shows a substrate-temperature dependent composition. Feldman, Sun, and Farabaugh[24] found nonbridging or superfluous oxygen existing in reactive-evaporated SiO$_x$ films. At higher temperatures, oxygen desorption is easier. Brodkorb *et al.*[25] also reported an increase in Si concentration with increasing substrate temperatures due to the desorption of the molecular component of the partially dissociated oxygen. Thus, the Si concentration in the films increases with increasing substrate temperatures.

For comparison, the XPS spectra of the PECVD SiO$_x$ films are shown in Fig. 7. The Si $2p$ spectra of the PECVD SiO$_x$ films display asymmetrical broad peaks which are continually shifted from 103.2 eV of Si^{4+} to lower binding energy with decreasing flow ratio R. The Si concentration in the films is found to increase accordingly. The broad and smooth peaks indicate a random-bonding or continuous-random-network structure of the PECVD SiO$_x$ films.

From the XPS spectra, the two apparent peaks for the SiO$_x$ films deposited by PLD, and one broad and smooth peak by PECVD, suggest that the films deposited by PLD show a nonuniform nanophase compared with those by PECVD. As the laser-induced plasma plume consists of a large amount of clusters and fragments, the SiO$_x$ films deposited by PLD show a nonuniform nanostructure. On the contrary, the growth in PECVD occurs at the atom-molecule level. With enough atom-molecule diffusion, the PECVD films show a random-bonding structure.

C. Optical absorption and photoluminescence of the deposited thin films

The optical absorption of the SiO$_x$ nanostructured films formed by PLD was characterized by UV-Vis. As the optical constants of the SiO$_x$ films are approximate to those of the quartz substrate due to high oxygen concentration in the
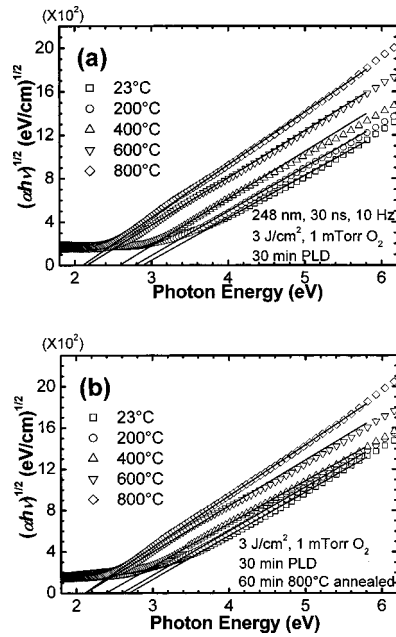
FIG. 8. Tauc plot, $(\alpha h\nu)^{1/2}$ vs $h\nu$ for the SiO_x nanostructured films deposited by PLD at different substrate temperatures. (a) As-deposited, (b) after 60 min high-vacuum annealing at a temperature of 800 °C.

films, the effect of multiple internal reflects of the air/film/substrate/air multilayers was neglected. The absorption coefficient α can be obtained through the following equation:[26]

$$T = \frac{(1-R)^2 e^{-\alpha d}}{1 - R^2 e^{-2\alpha d}}, \tag{1}$$

where T is the transmittance measured from UV-Vis, d is the film thickness, and R is the reflection coefficient measured in the weak absorption range ($\lambda = 1.3$ μm). The optical band gap E_{opt} can be estimated from the following relation, which is known as the Tauc plot,

$$\alpha h\nu = \text{const}(h\nu - E_{opt})^n, \tag{2}$$

where $h\nu$ is the photon energy and the exponent n has a value of 2 for an indirect transition.

Figure 8(a) shows the Tauc plot, $(\alpha h\nu)^{1/2}$ as a function of $h\nu$ for the as-deposited SiO_x nanostructured films. Approximately linear relations are observed. Intersecting points of the horizontal axis correspond to the optical band gap. With increasing substrate temperatures, the band gap is reduced from 2.9 to 2.1 eV on a continual basis. The absorption coefficient is enhanced with a steeper slope. Although substrate annealing took place due to the heated substrates during deposition, we can see below that the annealing alone does not have such a large impact on optical absorption. The evolution of the absorption spectra is due to the increased Si concentration in the films. According to the electronic structure of a-SiO_x, the band gap of a-SiO_2 is around 8.5 eV and that of a-Si is about 1.5 eV. The electronic states of a-SiO_2 near the valence band edge are derived from O nonbonding states. With x decreasing from 2.0 in a-SiO_x, the valence band edge moves up, as the introduced Si-Si bond states are gradually overlaid with the O nonbonding states and finally spread out into the Si valence band. Simultaneously, the con-

duction edge also moves down. The net result is that the band gap decreases nonlinearly as Si concentration increases.[21,27] The increased Si-related clusters as diffuser centers also cause the enhancement of the absorption coefficient.

Figure 8(b) shows the Tauc plot for the SiO_x nanostructured films after 60 min high-vacuum annealing at 800 °C. Compared with those of the as-deposited films, the absorption coefficient is increased, the slope becomes steeper, and the optical band gap is reduced. Furthermore, the optical absorption still shows the substrate-temperature dependence. During annealing, SiO_x starts to separate into its SiO_2 phase and Si clusters at a temperature of 400–700 °C. At temperatures lower than 800 °C, the SiO_x films are amorphous but display a certain amount of partial ordering in the amorphous structure.[28–30]

We also measured the Raman spectra of the SiO_x nanostructured films after annealing. The films show Raman spectra similar to those of as-deposited films, which confirms the amorphous state of the films. Thus, during annealing, mild phase separation and Si-atom agglomeration enhance the interaction between the Si-Si bonds, and the band gap decreases as well.

The physical mechanisms for the light emission from Si nanostructures have continually generated controversy. Some work suggests that surface states and surface alloys are the principal mechanisms leading to the light emission.[31] The widely used QCE theory explains the high efficiency light emission as a result of the band-to-band radiative recombination of electron-hole pairs confined in Si NCs whose surfaces are very well passivated by Si-H or Si-O bond.[32] There is also experimental evidence that amorphous species a-Si or a-SiO_x used to confine Si NCs can be responsible for the light emission.[33] The diverse or even contradictory experimental results in the literature suggest that the light emission from Si NCs has a multiple mechanism.

In our previous study,[17] we investigated the effects of deposition and thermal treatment conditions on the structures and PL properties of Si NCs formed by PLD. The peak shifts with different ambient gas pressure and blueshifts after oxidation or thermal annealing show that the red PL band at 1.8–2.1 eV is due to the QCE in Si NC cores. The fixed peak position relates the blue PL band at 2.55 eV to the localized surface states at the SiO_x/Si interface. Several authors also described two PL bands in the blue-green and yellow-red ranges from SiO_x.[34–36] They attributed the blue-green band to the carrier recombination at surface states or defects and the yellow-red band to the recombination of confined electron-hole pairs in Si NCs.

We studied the substrate-temperature dependence of PL from the SiO_x nanostructured films formed by PLD. Figure 9(a) shows the PL spectra of the SiO_x nanostructured films deposited at different substrate temperatures. The film deposited at 23 °C shows a broad PL band at ~1.9 eV. The asymmetric PL peak can be regarded as a superposition of two or three smaller peaks. The multiple peak could be caused by a nonuniform and highly asymmetric size distribution or discrete cluster size with atomic layer steps.[11,37] With increasing substrate temperatures, the PL is continually redshifted to
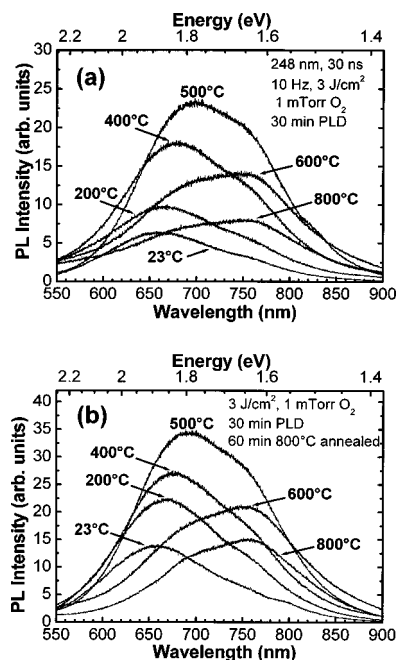
FIG. 9. PL of the SiO$_x$ nanostructured films deposited by PLD at different substrate temperatures. (a) As-deposited, (b) after 60 min high-vacuum annealing at a temperature of 800 °C.

~1.6 eV. The corresponding PL intensity shows an increase up to 500 °C and then decreases. The redshifted PL is in good agreement with the increased Si concentration, as the increased Si clusters and their size cause the lower energy PL. Therefore, the most plausible explanation of the PL band is QCE theory. The PL also shows consistency with the evolution of the optical band gap. As to the intensity variation, the PL intensity is determined not only by the number and dimension of Si clusters, but also the nonradiative defects and dangling bonds. The nonradiative recombination by defects and dangling bonds always competes with the radiative recombination, which gives rise to luminescence.

Figure 9(b) shows the PL spectra for the SiO$_x$ nanostructured films after 60 min high-vacuum annealing at 800 °C. All the films show PL with enhanced intensity but no peak shift. As discussed above, the thermally induced bonding modification is not severe at 800 °C. The PL position is only dependent on the film composition. The enhanced PL intensity is due to a better ordering of the amorphous films and the reduction of both defects and dangling bonds.

The optical band gaps and PL peak energies of the SiO$_x$ nanostructured films formed by PLD were summarized in Fig. 10. There is a clear correlation between the two optical properties. A considerable shift between the PL peak energy and the optical band gap can also be observed. Such a difference could be explained by the Brodsky's quantum well model.[38] The PL is believed to be the result of the recombination of electron-hole pairs in the Si well, while the optical band gap is determined by the electronic transition between extended states.[39]

The PL from the PECVD SiO$_x$ films was also studied. The as-deposited films show no PL. After high-vacuum annealing at temperatures ranging from 600 to 1200 °C, a strong visible PL shows enhanced intensity and a continuous
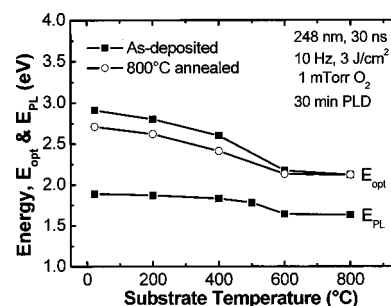

FIG. 10. Optical band gaps and PL peak energies of the SiO$_x$ nanostructured films formed by PLD.

redshift from 1.9 to 1.4 eV with increasing annealing temperature. Figure 11 shows the PL spectra of the SiO$_x$ films after 60 min high-vacuum annealing at 800 °C. A continuous redshift of the PL band at 1.9–1.6 eV can be observed with decreasing flow ratio R (or increasing Si concentration), which is in good agreement with the PLD results. Similarly, the decreased PL peak energy with increasing Si concentration suggests that the light emission could be due to the QCE. Iacona, Franzò, and Spinella[8] also reported that the red band PL from vacuum-annealed SiO$_x$ films continually redshifts with increasing Si concentration and annealing temperature. Based on strong correlation between structural and optical data, they concluded that the red PL from the SiO$_x$ films is due to the carrier recombination in Si NCs.

IV. CONCLUSIONS

SiO$_x$ nanostructured films were formed by PLD in O$_2$ gas at different substrate temperatures. After laser ablation, the single-crystal Si(100) target showed a polycrystal structure due to melting and recrystallization, and weak PL due to the cluster deposition and microstructure formation on the target surface. The strong PL at 1.6–1.9 eV was found to be from the amorphouslike background films. With increasing substrate temperatures, both the PL band and optical band gap continually redshift due to the increased Si concentration. After annealing at 800 °C, the PL and optical absorption are enhanced due to a better ordering and bonding of Si clusters in the films. The optical band gap also decreases after annealing due to the enhanced interaction between the Si-Si bonds. The annealed SiO$_x$ films deposited by PECVD showed continuous redshifts of PL with decreasing flow ratio
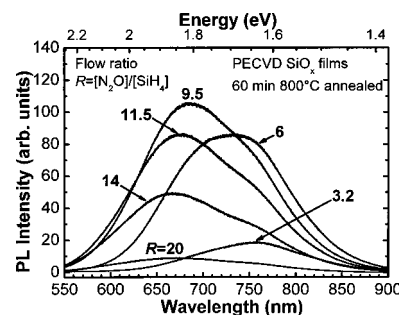

FIG. 11. PL of the SiO$_x$ films deposited by PECVD at different values of flow ratio $R=[N_2O]/[SiH_4]$ after 60 min high-vacuum annealing at a temperature of 800 °C.

R (or increasing Si concentration). The good agreement of PL peak energy with Si concentration from both the PLD and PECVD results supported our conclusion that the origin of the light emission is due to the QCE.

ACKNOWLEDGMENTS

[1] S. Furukawa and T. Miyasato, Jpn. J. Appl. Phys., Part 2 **27**, L2207 (1988).

[2] H. Takagi, H. Ogawa, Y. Yamazaki, A. Ishizaki, and T. Nakagiri, Appl. Phys. Lett. **56**, 2379 (1990).

[3] L. T. Canham, Appl. Phys. Lett. **57**, 1046 (1990).

[4] M. Ehbrecht, H. Ferkel, F. Huisken, L. Holz, Y. N. Polivanov, V. V. Smirnov, O. M. Stelmakh, and R. Schmidt, J. Appl. Phys. **78**, 5302 (1995).

[5] T. S. Iwayama, S. Nakao, and K. Saitoh, Appl. Phys. Lett. **65**, 1814 (1994).

[6] G. Belomoin *et al.*, Appl. Phys. Lett. **80**, 841 (2002).

[7] A. Nakajima, Y. Sugita, K. Kawamura, H. Tomita, and N. Yokoyama, Jpn. J. Appl. Phys., Part 2 **35**, L189 (1996).

[8] F. Iacona, G. Franzò, and C. Spinella, J. Appl. Phys. **87**, 1295 (2000).

[9] E. Werwa, A. A. Seraphin, L. A. Chiu, C. Zhou, and K. D. Kolenbrander, Appl. Phys. Lett. **64**, 1821 (1994).

[10] T. Makino, Y. Yamada, N. Suzuki, T. Yoshida, and S. Onari, J. Appl. Phys. **90**, 5075 (2001).

[11] L. Patrone, D. Nelson, V. I. Safarov, M. Sentis, and W. Marine, J. Appl. Phys. **87**, 3829 (2000).

[12] T. Makimura, Y. Kunii, N. Ono, and K. Murakami, Jpn. J. Appl. Phys., Part 2 **35**, L1703 (1996).

[13] D. H. Lowndes, C. M. Rouleau, T. Thundat, G. Duscher, E. A. Kenik, and S. J. Pennycook, Appl. Surf. Sci. **127–129**, 355 (1998).

[14] I. Umezu, K. Shibata, S. Yamaguchi, A. Sugimura, Y. Yamada, and T. Yoshida, J. Appl. Phys. **84**, 6448 (1998).

[15] D. B. Geohegan, A. A. Puretzky, G. Duscher, and S. J. Pennycook, Appl. Phys. Lett. **72**, 2987 (1998).

[16] L. Y. Chen, in *Pulsed Laser Deposition of Thin Films*, edited by D. B. Chrisey and G. K. Hubler (Wiley, New York, 1994), p. 186.

[17] X. Y. Chen, Y. F. Lu, Y. H. Wu, B. J. Cho, M. H. Liu, D. Y. Dai, and W. D. Song, J. Appl. Phys. **93**, 6311 (2003).

[18] B. Luk'yanchuk, W. Marine, S. Anisimov, and G. Simakina, Proc. SPIE **3618**, 434 (1999).

[19] H. C. Le, R. W. Dreyfus, W. Marine, M. Sentis, and I. A. Movtchan, Appl. Surf. Sci. **96–98**, 164 (1996).

[20] T. I. Campbell and P. Fauchet, Solid State Commun. **58**, 739 (1986).

[21] F. G. Bell and L. Ley, Phys. Rev. B **37**, 8383 (1988).

[22] S. Hayashi, S. Tanimoto, and K. Yamanoto, J. Appl. Phys. **68**, 5300 (1990).

[23] B. H. Augustine, E. A. Irene, Y. J. He, K. J. Price, L. E. McNeil, K. N. Christensen, and D. M. Maher, J. Appl. Phys. **78**, 4020 (1995).

[24] A. Feldman, Y. N. Sun, and E. N. Farabaugh, J. Appl. Phys. **63**, 2149 (1988).

[25] W. Brodkorb, J. Salm, C. Steinbeiss, and E. Steinbeiss, Phys. Status Solidi A **57**, 49 (1980).

[26] J. I. Pankove, *Optical Processes in Semiconductors* (Dover, New York, 1975), p. 412.

[27] A. I. Bennett and L. M. Roth, Phys. Rev. B **4**, 2686 (1971).

[28] B. J. Hinds, F. Wang, D. M. Wolfe, C. L. Hinkle, and G. Lucovski, J. Vac. Sci. Technol. B **16**, 2171 (1998).

[29] U. Kahler and H. Hofmeister, Appl. Phys. Lett. **75**, 641 (1999).

[30] D. Nesheva, C. Raptis, A. Perakis, I. Bineva, Z. Aneva, Z. Levi, S. Alexandrova, and H. Hofmeister, J. Appl. Phys. **92**, 4678 (2002).

[31] F. Koch, V. Petrova-Koch, and T. Muschik, J. Lumin. **57**, 271 (1993).

[32] B. Delley and E. F. Steigmeier, Phys. Rev. B **47**, 1397 (1993).

[33] S. M. Prokes, Appl. Phys. Lett. **62**, 3244 (1993).

[34] A. J. Kenyon, P. F. Trwoga, C. W. Pitt, and G. Rehm, J. Appl. Phys. **79**, 9291 (1996).

[35] S. Tong, X.-N. Liu, T. Gao, and X.-M. Bao, Appl. Phys. Lett. **71**, 698 (1997).

[36] L. Khomenkova *et al.*, J. Lumin. **102-103**, 705 (2003).

[37] R. Behrensmeier, F. Namavar, G. B. Amisola, F. A. Otter, and J. M. Galligan, Appl. Phys. Lett. **62**, 2408 (1993).

[38] M. H. Brodsky, Solid State Commun. **36**, 55 (1980).

[39] J. L. Yeh and S. C. Lee, J. Appl. Phys. **79**, 656 (1996).